REFLECTANCE MEASUREMENTS ON EUROPIUM-DOPED LANGASITE, LANGANITE AND LANGATATE POWDERS

S. GEORGESCU, A. M. VOICULESCU, C. MATEI. O. TOMA, L. GHEORGHE, A. ACHIM

National Institute for Laser, Plasma and Radiation Physics, Magurele, Romania

Abstract. In order to compare the red luminescence efficiency of europium-doped langasite, langanite and langatate when pumped in various f-f absorption bands, reflectance measurements on powders are performed in the 350–650 nm wavelength domain. The langanite and langatate crystals show brighter luminescence than the langasite.

Key words: reflectance, langasite, langanite, langatate, europium.

1. INTRODUCTION

The crystals from the langasite family were initially intended as hosts for laser active media [1], but in present their main application is based on their very good piezoelectric characteristics [2, 3]. Nowadays, langasite ($La_3Ga_5SiO_{14}$ - LGS) tends to replace quartz in high temperature applications [4]. Also, langasite is used for electro-optic Q-switch [5], for gas sensor [6], and so on. Recently, selftuning of Nd^{3+} in langasite crystals was obtained [7].

Two other members of the langasite family, langanite ($La_3Ga_{5.5}Nb_{0.5}O_{14}$ − LGN) and langatate ($La_3Ga_{5.5}Ta_{0.5}O_{14}$ − LGT) proved to have superior characteristics in some applications [8]. LGS, LGN and LGT are partially disordered crystals, i.e., one of the crystallographic positions is shared by two different ions. This results in inhomogeneously broadened absorption and fluorescence lines which was first considered an advantage for laser emission: wider absorption lines result in an efficient pumping while wider emission lines means tunability.

LGS, LGN and LGT crystallize in the *P321* space group, symmetry class *32* and are isostructural with the calciumgallogermanate ($Ca_3Ga_2Ge_4O_{14}$) [9]. The general formula is $A_3BC_3D_2O_{14}$, where *A* represents the dodecahedral positions (distorted Thompson cubes), *B* − octahedral positions and *C, D* − tetrahedral positions. La^{3+} occupies the position *A*. The local symmetry at this site is C_2 [10]. In contrast with LGS where Ga^{3+} and Si^{4+} share with equal probability the

tetrahedral positions D, in LGN (LGT) the octahedral positions B are occupied by two different ions, Ga^{3+} and Nb^{3+} (Ta^{5+}) (also, with equal probability). Ga^{3+} occupies the remaining positions (C and D). The structural difference between LGS and LGN (or LGT) consists in the placement of the shortest distance positions randomly occupied around the A site: four positions in the plane perpendicular on the C_2 axis for LGS and two positions along the C_2 axis in LGN and LGT. Besides, there is a larger charge difference between Nb^{5+} (or Ta^{5+}) and Ga^{3+} than between Si^{4+} and Ga^{3+} [11].

When excited in the near UV (396 nm, transition $^7F_0 \rightarrow {}^5L_6$), both Eu^{3+}-doped LGS and LGT crystals show bright red luminescence which suggests the possibility to use these materials as red phosphors. In this paper we use the reflectance measurements to compare the absorption and emission characteristics of Eu^{3+} doped in LGS, LGN and LGT powders. The main advantage of the reflectance measurements performed in this paper is the presence, on the same record, of both f-f absorption and emission bands.

2. EXPERIMENTAL

Eu-doped langasite, langanite and langatate were synthesized in our laboratory from high-purity La_2O_3, Ga_2O_3, SiO_2, Nb_2O_5, Ta_2O_5, Eu_2O_3, according to $(La_{0.95}Eu_{0.05})_3Ga_5SiO_{14}$ and, respectively, $(La_{0.97}Eu_{0.03})_3Ga_{5.5}Nb_{0.5}O_{14}$ and $(La_{0.97}Eu_{0.03})_3Ga_{5.5}Ta_{0.5}O_{14}$ formulae. The oxides were mixed in an agate balls mill and calcinated at 1500ºC for 24 h. The powder was pressed in pallets and the crystals were grown along the C-axis in platinum crucibles in nitrogen atmosphere, using the Czochralski method. The powders of Eu^{3+} doped LGS, LGN and LGT were obtained by milling of single crystals.

A near parallel light beam from a W-halogen lamp was projected normally on the quartz cuvette containing the powder (Fig. 1). The reflected light was collected with a concave mirror and projected on the entrance slit of a Jobin-Yvon 1000M monochromator equipped with an S-20 photomultiplier. The signal was processed by a SR830 lock-in amplifier online with a computer. The reflectance spectra were recorded in the 350-650 nm spectral domain which corresponds to the main f-f absorption bands as well as to the main ($^5D_0 \rightarrow {}^7F_2$) emission band. For comparison, the reflectance spectrum of MgO powder is recorded.

3. RESULTS AND DISCUSSION

The samples, contained in quartz cuvettes, are illuminated with white light from a W-halogen lamp. The experimental apparatus is sketched in Fig. 1. The white light from the W-halogen lamp is focused on the sample. The reflected light is collected by the concave mirror and projected on the entrance slit of the

monochromator. The light reflected by the cuvette passes through the mirror's hole and is not recorded. A stop is placed behind the cuvette (not shown in Fig. 1); thus, only the reflected light (contained in the solid angle Φ allowed by the mirror) reaches the entrance slit.

In contrast with the usual reflectance measurements, the sample is placed before the monochromator and receives white light. In fact, we note that our measurements are not true diffuse reflectance ones. Nevertheless, only the contribution of diffused light (contained in the solid angle Φ) is recorded. The specular reflection is avoided due to the mirror's hole. Part of the incident light is absorbed by the material (an overall contribution due to the crystal host and the contribution of the Eu^{3+}-narrow bands). Due to the specific illumination conditions, the light absorbed by the Eu^{3+} excites its luminescence. Therefore, besides the specific (in our case, f-f) absorption bands, in the recorded spectrum the luminescence bands can be observed.
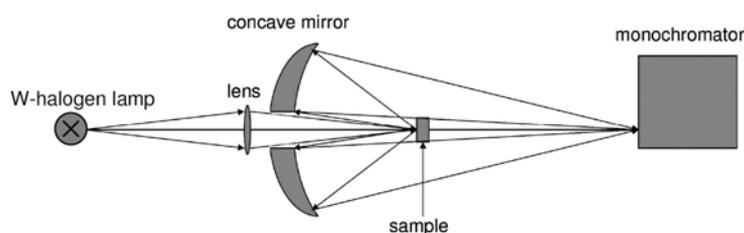

Fig. 1 − Sketch of the experimental set-up used for reflectance measurements.

The strongest luminescent transition of Eu^{3+} in LGS, LGN and LGT [12] is $^5D_0 \rightarrow {}^7F_2$. Because this transition ends on a level which is not populated at room temperature, the inverse transition ($^7F_2 \rightarrow {}^5D_0$, absorption) cannot be observed and the emitted luminescence is not re-absorbed. This is not the case when the terminal level is the ground one ($^7F_0$). For example, the transition between $^5D_0$ and $^7F_0$ is observed in absorption.

The reflectance spectra of Eu-doped LGS, LGN and LGT powders (together with the MgO powder as reference for white), in the spectral domain 350-650 nm, are given in Fig. 2. The shape of these curves reflects the spectral sensitivity of both monochromator grating (blazed for 500 nm) and of the photomultiplier (S-20 spectral response) as well as the emission characteristics of the W-halogen lamp (~ 3000K color temperature). The available spectral domain is limited toward short wavelengths mainly due to the emission of the W-halogen lamp. Therefore, the UV domain characteristic for the charge-transfer bands is not accessible in our experiments. Nevertheless, the main f-f absorption bands (including $^7F_0 \rightarrow {}^5L_6$, at ~ 396 nm) are found in this domain.
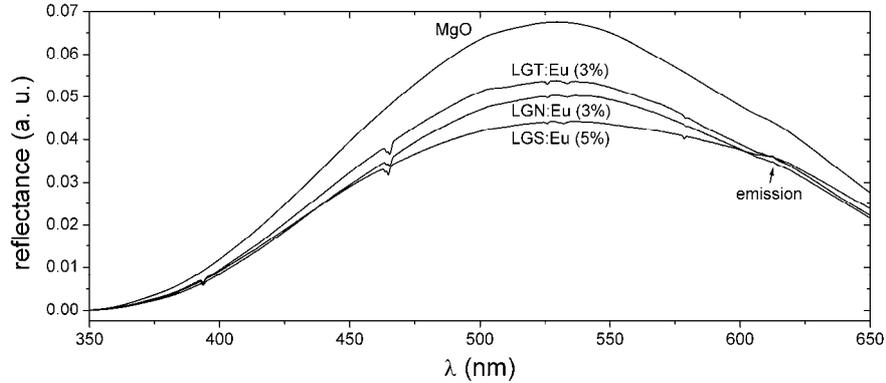
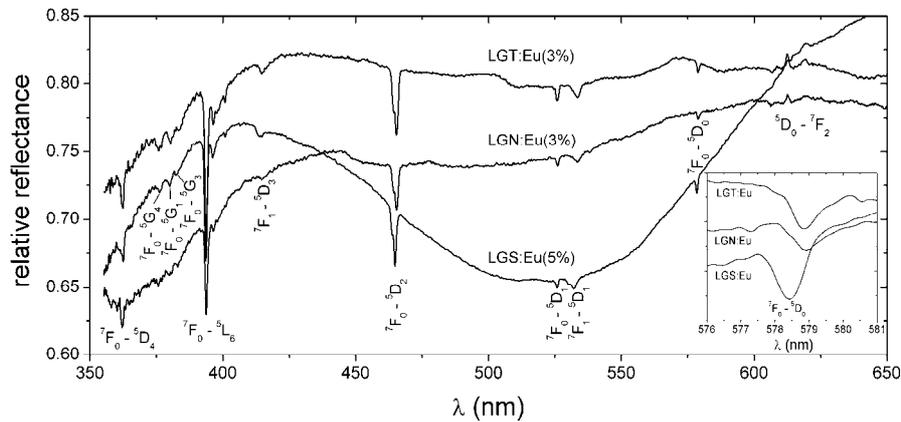Fig. 2 – Reflectance spectra of LGS:Eu, LGN:Eu, LGT:Eu and MgO powders.

Fig. 3 – Relative reflectance (in rapport with MgO) of LGS:Eu, LGN:Eu, LGT:Eu powders. Both absorption and emission transitions are identified. Inset: transition $^7F_0 \rightarrow {}^5D_0$; for an easier comparison, the base lines in the inset were slightly modified.

Even in the scale of Fig. 2, the absorption bands characteristic to the f-f transitions of Eu^{3+} can be seen. The emission lines for Eu-doped LGN and LGT could be observed as a small feature at ~ 613 nm. Both absorption and emission Eu^{3+} lines become more visible in Fig. 3 where the relative reflectance spectra, obtained by dividing the LGS, LGN and LGT reflectance spectra to the MgO powder one, are shown. The general shape of these spectra depends on the reflectance peculiarities of the crystal host.

An inspection of the relative reflectance spectra from Fig. 3 shows that the position of the f-f absorption bands is red shifted in both LGN and LGT compared to LGS. Details concerning the red shift of the transition $^7F_0 \rightarrow {}^5D_0$ are given in the inset of Fig. 3. The red shift observed in the Eu^{3+} luminescence in LGT compared

to LGS was explained by a more covalent Eu^{3+} - O^{2-} bond in LGT [12, 13]. Approximately the same red shift is observed in the relative reflectance spectrum of Eu^{3+} in LGN. This is not surprising, taking into account that LGN and LGT have the same structure and Nb^{5+} has the same ionic radius as Ta^{5+} [14].

Fig. 3 allows, also, a qualitative comparison of the emission efficiency of Eu-doped LGS, LGN and LGT powders. Thus, though the europium concentration is higher in LGS, the features, representing the luminescence lines of the transition $^5D_0 \rightarrow {}^7F_2$ of Eu^{3+} are more evident in LGN and LGT.

4. CONCLUSIONS

The reflectance spectra performed in this paper put in evidence, on the same record, absorption and emission ($^5D_0 \rightarrow {}^7F_2$) lines of Eu^{3+} in LGS, LGN and LGT powders. The analysis of the relative reflectance spectra (divided by the MgO reflectance) have shown the same red shift of the absorption lines of Eu^{3+} in LGN and LGT compared with LGS, explained by a higher degree of covalence in the first two materials. Besides, the relative reflectance spectra allow a qualitative comparison of the emission efficiency which favors LGN and LGT.

REFERENCES

1. A. A. Kaminskii, I. M. Silvestrova, S. E. Sarkisov, G. A. Denisenko, *Investigation of trigonal (La$_{1-x}$ Nd$_x$)$_3$Ga$_5$SiO$_{14}$ crystals. II. Spectral laser and electrochemical properties*, Phys. Stat. Solid A, **80**, 607–620 (1983).
2. J. Détaint, J. Schwartzel, A. Zarka, B. Capelle, J. P. Denis, E. Phillipot, *Bulk wave propagation and energy trapping in the new thermally compensated materials with trigonal symmetry*, Proc. IEEE Internat. Frequency Control Symposium, 1994, pp. 58–71.
3. R. C. Smythe, R. C. Helmbold, G. E. Hague, K. A. Snow, *Langasite, Langanite, and Langatate Bulk-Wave Y-Cut Resonators*, IEEE Trans. UFFC, **47**, 2000, pp. 355–360.
4. H. Fritze, H. Seh, H. L. Tuller, G. Borchardt, *Operation limits of langasite high temperature nanobalances*, J. Eur. Ceram. Soc., **21**, 1473–1477 (2001).
5. H. Kong, J. Wang, H. Zhang, X. Yin, S. Zhang, Y. Liu, X. Cheng, L. Gao, X. Hu, M. Jiang, *Growth, properties and application as an electrooptic Q-switch of langasite crystal*, Cryst. Growth, **254**, 360–367 (2003).
6. H. Seh, H. L. Tuller, H. Fritze, Sensor Actuat. B, *Langasite for high-temperature acoustic wave gas sensors*, **93**, 169–174 (2003).
7. I. Aramburu, I. Iparraguirre, M. A. Illarramendi, J. Azkargorta, J. Fernandez, R. Balda, *Self-tuning in birefringent La$_3$Ga$_5$SiO$_{14}$: Nd^{3+} laser crystal*, Opt. Mat., **27**, 1692-1696 (2005).
8. B. Chai, H. Qiu, Y. Y. Ji, J. L. Lefaucheur, *Growth of high quality single domain crystals of langasite family compounds*, Proc. IEEE Internat. Frequency Control Symposium, 1999, pp. 821–828.

9. B. V. Mill, A. V. Butashin, G. G. Kodzhabagian, E. L. Belokoneva, N. V. Belov, *Modified rare-earth gallates with the structure of $Ca_3Ga_2Ge_4O_{14}$*, Doklady Akademii Nauk SSSR, **264**, 1385–1389 (1982).

10. V. N. Molchanov, B. A. Maksimov, A. F. Kondakov, T. S. Chernaya, Yu. V. Pisarevsky, V. I. Simonov, *Crystal structure and optical activity of $La_3Nb_{0.5}Ga_{5.5}O_{14}$ and $Sr_3Ga_2Ge_4O_{14}$ single crystals of the langasite family*, JETP Lett., **74**, 222–225 (2001).

11. S. Georgescu, O. Toma, A. Achim, A. M. Chinie, L. Gheorghe, A. Stefan, *Optical studies of the partially disordered crystals langasite ($La_3Ga_5SiO_{14}$) and langatate ($La_3Ga_{5.5}Ta_{0.5}O_{14}$) doped with Eu^{3+}*, Proc. SPIE, Vol. 6785, 2007, p. 6785–9.

12. S. Georgescu, O. Toma, A. M. Chinie, L. Gheorghe, A. Achim, A. S. Stefan, *Spectroscopic characteristics of langasite ($La_3Ga_5SiO_{14}$) and langatate ($La_3Ga_{5.5}Ta_{0.5}O_{14}$) crystals doped with Eu^{3+}*, Opt. Mat., **30**, 1007–1012 (2008).

13. S. Georgescu, O. Toma, A. M. Chinie, L. Gheorghe, A. Achim, A. S. Stefan, *Excited state dynamics of Eu^{3+} in the partially disordered crystals $La_3Ga_5SiO_{14}$ and $La_3Ga_{5.5}Ta_{0.5}O_{14}$*, J. Lumin., **128**, 741–743 (2008).

14. R. D. Shannon, *Revised effective ionic radii and systematic studies of interatomic distances in halides and chalcogenides*, Acta Cryst. A, **32**, 751–767 (1976).